JMEPEG (2017) 26:366–373
DOI: 10.1007/s11665-016-2426-4

Substrate Frequency Effects on Cr_xN Coatings Deposited by DC Magnetron Sputtering

Aleksei Obrosov, Muhammad Naveed, Alex A. Volinsky, and Sabine Weiß

(Submitted January 27, 2016; in revised form October 28, 2016; published online November 16, 2016)

Controlled ion bombardment is a popular method to fabricate desirable coating structures and modify their properties. Substrate biasing at high frequencies is a possible technique, which allows higher ion density at the substrate compared with DC current bias. Moreover, high ion energy along with controlled adatom mobility would lead to improved coating growth. This paper focuses on a similar type of study, where effects of coating growth and properties of DC magnetron-sputtered chromium nitride (Cr_xN) coatings at various substrate bias frequencies are discussed. Cr_xN coatings were deposited by pulsed DC magnetron sputtering on Inconel 718 and (100) silicon substrates at 110, 160 and 280 kHz frequency at low duty cycle. Coating microstructure and morphology were studied by X-ray diffraction (XRD), atomic force microscopy (AFM), scanning electron microscopy (SEM), scratch adhesion testing and nanoindentation. Results indicate a transformation of columnar into glassy structure of Cr_xN coatings with the substrate bias frequency increase. This transformation is attributed to preferential formation of the Cr_2N phase at high frequencies compared with CrN at low frequencies. Increase in frequency leads to an increase in deposition rate, which is believed to be due to increase in plasma ion density and energy of the incident adatoms. An increase in coating hardness along with decrease in elastic modulus was observed at high frequencies. Scratch tests show a slight increase in coating adhesion, whereas no clear increase in coating roughness can be found with the substrate bias frequency.

Keywords adhesion of coatings, CrN coatings, frequency, mechanical properties, microstructure, PVD, X-ray diffraction

1. Introduction

Pulsed magnetron sputtering process is one of the most significant developments in physical vapor deposition (PVD) technology in the 1990s and a well-established technique for the fabrication of thin films and coatings (Ref 1, 2). Moreover, this method has been recently used as an alternative method to sinusoidal bias, as it overcomes charge accumulation induced by incident ions and controls the energy of the ions coming towards the substrate. By controlling the duty cycle (the ratio of the pulse-on to pulse-off time), the shape of a pulse can be modified, leading to better arc management process during coating deposition. High thermal flux with the increase in substrate pulse frequency has also been reported by Kelly (Ref 3). Microstructure and properties of the coatings can be modified by controlling the ion flux on the substrate surface (Ref 4). Increase in the ion flux provides higher bombardment, thus modifying film properties, such as microstructure, mechanical properties, film density and adhesion (Ref 5, 6).

Chromium nitride (Cr_xN) coatings are well-known candidates, which are often used for tribological, material forming and casting applications (Ref 7-10), as they exhibit high hardness, good wear and corrosion resistance, high thermal stability, superior fracture toughness, etc. (Ref 8, 11-13). A number of publications have been discussing the fabrication of Cr_xN films using DC and pulsed bias. Freeman et al. (Ref 7) found that Cr_xN harder films with higher internal stresses and denser microstructure are produced with pulsed bias compared with DC magnetron sputtering. Similarly, Lin et al. (Ref 14) reported a change in preferred orientation of the coatings during fabrication of Cr-Al-N at various substrate frequencies. Moreover, they found higher internal stresses along with better mechanical properties of the coatings fabricated at higher frequencies. They associated these effects with the energy and ion flux observed at the substrate during the deposition process. Similarly, Lee et al. (Ref 15) found a variation in preferred orientation, microstructure and mechanical properties of Cr_xN thin films deposited with various frequencies in the 2-80 kHz range.

Literature reports hint to high ion energy, low negative sputtering and high positive sputtering at 110-350 kHz frequency (Ref 14). Moreover, such coatings exhibit high hardness and good tribological properties. Bradly et al. (Ref 16) performed Langmuir measurements and showed an increase of 28% in ion flux between 110 and 350 kHz, enabling high deposition rates with high energy electrons. They also demonstrated that high frequency of approximately 350 kHz at low duty cycles could be beneficial for optimum plasma conditions. Khaesh et al. (Ref 17) obtained small grain size at 120 kHz, which leads to denser coatings and good mechanical properties. However, no study has been performed discussing the effect of substrate bias frequency in the range between 110 and 280 kHz at low duty cycle. The present work

Aleksei Obrosov, Muhammad Naveed, and **Sabine Weiß**, Chair of Physical Metallurgy and Materials Technology, Brandenburg Technical University, Konrad Wachsmann Allee 17, 03046 Cottbus, Germany; and **Alex A. Volinsky**, Department of Mechanical Engineering, University of South Florida, 4202 E. Fowler Ave., ENB118, Tampa, FL 33620, USA. Contact e-mail: aleksei.obrosov@b-tu.de.

shows the effects of the above discussed parameters on microstructure, mechanical properties and the phase transformation in Cr_xN films.

2. Experimental

Cr_xN coatings were produced using DC magnetron sputtering in the CC800/9 chamber from CemeCon AG (Würselen, Germany). The coatings were deposited onto 30 × 15 × 3 mm Inconel 718 substrates and (100) silicon wafers. Prior to deposition, Inconel 718 substrates were mirror polished and then cleaned in acetone. High-purity chromium target (99.99%) from PLANSEE AG (Reutte, Austria) was used for deposition, and the substrate-to-target distance was kept at approximately 70 mm. Deposition temperature was 550 °C, and 2 kW target power was used for the coating process. Substrate was biased at 90 V for the experiments with a constant duty cycle of 45%. Parameters for substrate frequency are summarized in Table 1.

Film thickness was measured using the CemeCon AG (Würselen, Germany) calowear test machine. Deposition rate of the coatings was estimated from the film thickness and deposition time. SEM images were obtained on the cross sections of films deposited on (100) Si wafers using TESCAN scanning electron microscope (Brno, Czech Republic). Additionally, chemical composition was determined by wavelength-dispersive X-ray spectroscopy (WDS). Mechanical properties (hardness and elastic modulus) of the coatings were estimated by using the Oliver and Pharr method (Ref 18) from the loading and unloading curves using a nanoindenter (UNAT) from ASMEC GmbH (Radeberg, Germany). Berkovich indenter with a maximum load of 10 mN has been used, which allowed a maximum 10% penetration depth of the film thickness (Ref 19, 20). An average of twenty measurements has been taken for the analysis.

Crystallographic phases and orientation of the films were identified by means of the grazing incidence X-ray diffraction (GIXRD) at a low incident angle of 9° with a Cu Kα source (λ = 0.15406 nm), operating at 40 kV and 40 mA. Surface topography of the coatings was examined using contact mode atomic force microscopy (AFM) from Nanosurf GmbH (Langen, Germany). CSM Instruments (Switzerland) Revetest scratch tester was used to investigate the adhesion between the coating and the substrate. Berkovich indenter with a radius of 200 nm was drawn across the coating surfaces under increasing normal load. The load was increased gradually starting from zero to 60 mN to determine the critical load. These critical load values represent an average of three measurements, performed under identical experimental conditions. The scratch traces on the film surface were analyzed using optical and scanning electron microscopy.

3. Results and Discussion

3.1 Influence of the Substrate Frequency on Current

It is a known fact that the ion current saturates after a particular value of voltage is achieved at the substrate (Ref 21). This saturation of current at the substrate leads to high collision repulsion of ions approaching the substrate, influencing the coating properties. Hence, pulse bias at the substrate can be introduced to avoid saturation of ion current, even at higher voltage (Ref 22). Langmuir investigations show that pulsing of the substrate bias leads to higher electron temperature and an increase in ion saturation by more than 2-3 times compared with constant bias. This also leads to higher ion-to-atom ratio with heat input at the substrate (Ref 23). The present study discusses pulsed substrate biasing to improve adhesion between the coating and the substrate. The process of substrate biasing has been performed using PINNACLE PLUS pulse generator from Advance Energy (San Jose, CA, USA). Various frequencies have been used for the experiments with a maximum constant duty cycle of 45%, which resulted in low surface roughness, high deposition rate and good mechanical properties (Ref 24). Low defect formation during growth, uniform coating thickness over a large substrate area and high coating adhesion at low substrate temperatures are identified as some of the advantages of using substrate bias frequency (Ref 25).

A relationship between the measured current at various frequencies is shown in Fig. 1. A rapid increase in substrate current occurs in the frequency range between 110 and

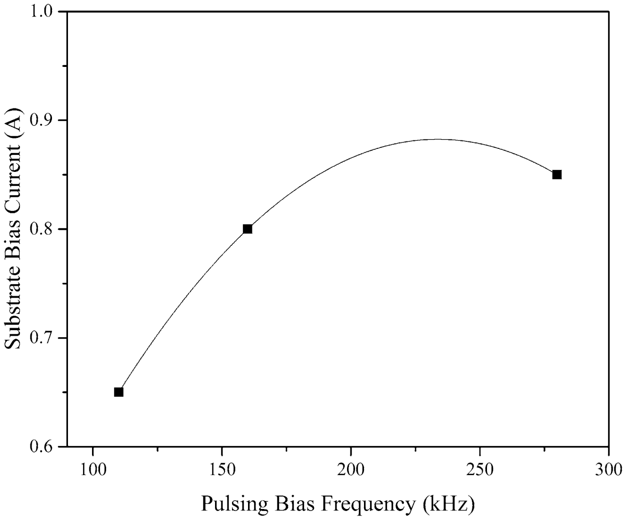

Fig. 1 Substrate bias current as a function of frequency during Cr_xN coatings deposition

Table 1 Deposition parameters of CrN coatings at various substrate bias frequencies

Coating	Deposition time, min	Pulsing parameters at the substrate, kHz	Cathode power, W	Pressure, mPa	N_2/Ar ratio	Bias, V
Argon etching	30	350	0	0.35	…	650
CrN	30	110	2000	0.3	0.23	90
CrN	30	160	2000	0.3	0.23	90
CrN	30	280	2000	0.3	0.23	90

160 kHz. A total increase of about 35% of the current has been obtained between the minimum and the maximum values of the substrate frequency, while the ion current values do not show saturation during pulsed biasing. Kelly et al. (Ref 22) found that the current during DC pulsed bias at 100-350 kHz is much higher than at constant DC bias. Similar increase in current with frequency is described for the deposition of TiO_2 films. In contrast to this, Bhaduri et al. (Ref 29) indicated that ion current declines with bias frequency at 70 V. Nevertheless, they identified that during the etching process at 500 V, the substrate ion current increased with frequency.

3.2 XRD and Chemical Analysis

Phase analysis was performed by means of X-ray diffraction measurements (XRD, Fig. 2). XRD results indicate a variation in the phase formation with changing bias frequency. As seen from the diffractograms, the Cr_xN films contain a mixture of hexagonal Cr_2N and cubic CrN phases. Film deposited at 110 kHz shows CrN (111), (220) and Cr_2N (111) X-ray reflections without preferred orientation. At 160 kHz frequency, a comparatively higher (111) intensity of Cr_2N can be seen. High intensities refer to preferential orientation and high texture coefficients of the coatings. Further intensification of the Cr_2N and reduction of the CrN (111) reflection intensity take place at 280 kHz. Additionally, an increase in bias frequency resulted in diffraction peaks shift at higher angles, indicating compressive residual stresses in these coatings (Ref 26).

Moreover, with the increase in substrate frequency, the CrN (111) peak disappeared along with intensification of the Cr_2N (111) diffraction peak. This demonstrates the possibility of coating texture control by varying substrate bias frequency. This phase transformation with varying process parameters can be associated with the surface energy change observed during the deposition process. During the deposition of Cr_xN planes, there is a high possibility of the (200) planes formation during initial deposition as they tend to orient themselves in monolayers inheriting lowest surface energy. During the later deposition stages, these adatoms orient themselves in the form of islands, transforming the coating preferential orientation from (200) to (111). Hence, a variation in preferred orientation can be observed with the increase in film thickness (Ref 27).

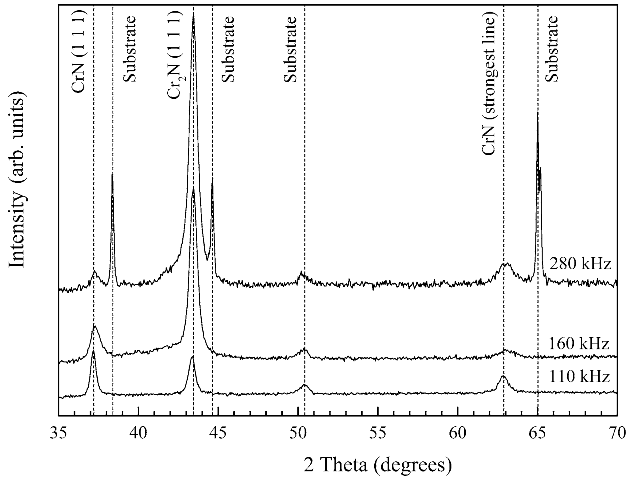

Fig. 2 XRD analysis of Cr_xN coatings deposited at different frequencies

WDS analysis shows an increase in Cr content with the substrate frequency. In contrast, a decrease in N content was measured due to the substrate frequency increase (Table 2). All Cr_xN coatings were found to be sub-stoichiometric with a Cr/N ratio ranging from 1.3 to 1.5. During the deposition process, metal ions eject from the target surface and collide with N to form respective nitrides. Although it can be seen from these measurements that at higher frequencies larger amount of Cr is available than at lower frequencies, this information is not sufficient to discuss the formation of CrN or Cr_2N at these process parameters and draw a direct correlation between WDS and XRD measurements. Langmuir probe analysis can be a possible method to determine the energy of ions at the substrate and discuss the formation of possible phases during the deposition process, but such measurements are not a part of this work.

3.3 Coating Structure and Deposition Rates

Cross-sectional morphology of Cr_xN coatings deposited on Si (100) substrates at 110, 160 and 280 kHz was studied by SEM and is presented in Fig. 3.

Table 2 WDX measurements obtained for Cr_xN coatings at various frequencies

	Pulsing parameters, kHz		
Element (at.%)	**110**	**160**	**280**
Cr	55.96	57.36	60.95
N	44.04	42.49	39.05

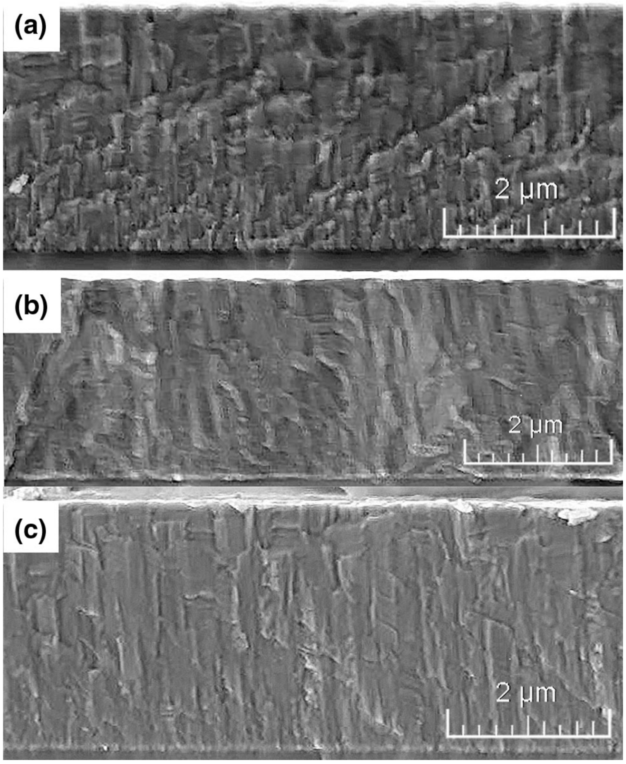

Fig. 3 Cross sections of Cr_xN films deposited at: (a) 110 kHz, (b) 160 kHz and (c) 280 kHz

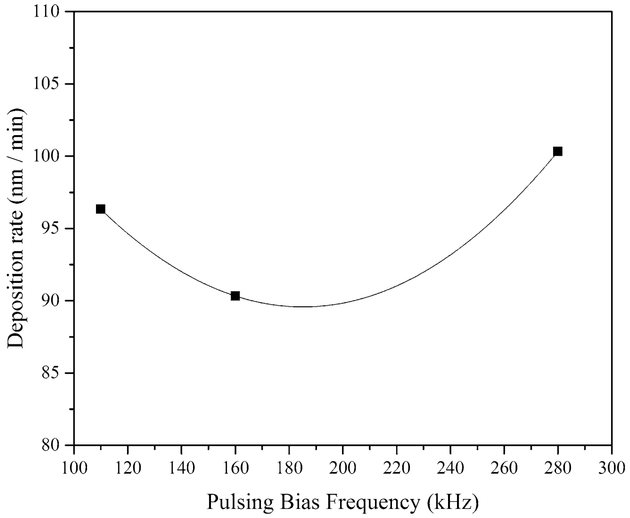

Fig. 4 Deposition rate of $\mathbf{Cr_xN}$ coatings, as a function of frequency

At 110 kHz a clear dense columnar structure of Cr_xN can be seen in Fig. 3(a), whereas at 160 kHz a smooth glass-like structure can be seen from the SEM image in Fig. 3(b). Similarly, a dense structure can also be observed for 280 kHz in Fig. 3(c), which seems to be denser than the other films. This change of structure might be attributed to the increase in electron temperature and a change in ion-to-atom ratio due to variation in process parameters (Ref 1). Another possible reason could be the change of the crystalline structure from CrN to Cr_2N at higher bias frequency due to higher mean energy of the ions approaching the substrate (Ref 28). XRD analysis of Cr_xN also supports the above mentioned theory, as a shift in preferred orientation can be seen from CrN to Cr_2N in Fig. 2.

Figure 4 shows the relationship between the frequency and the deposition rate of the Cr_xN coatings. The deposition rate remains almost constant. Change in frequency at the substrate allows high density of electrons on the substrate, resulting in high ionization rates, leading to more ions deposited on the surface. Bhaduri et al. (Ref 29) indicated that higher frequency led to increased film thickness. In contrast, Lee et al. (Ref 30) found a rapid decrease in deposition rate with the substrate bias frequency increase. At 160 kHz, the lowest thickness of the Cr_xN coating was found.

3.4 Mechanical Properties

Relationships between pulsing bias frequency, hardness and elastic modulus of Cr_xN films are given in Fig. 5. According to the literature, typical microhardness values of the Cr_xN films are between 11 and 30 GPa (Ref 15, 31, 32) depending on the coatings deposition method, process parameter, phase formation etc.

A decrease in elastic modulus of Cr_xN coatings can be seen with the substrate frequency. Contrarily, hardness of the coatings shows an increase at higher frequencies. These results can be correlated with the change in preferred orientation with increasing bias frequency. As Cr_2N phase was found to be preferential at higher frequencies, it is believed to have better mechanical properties compared with CrN (up to 28 GPa hardness) (Ref 33, 34).

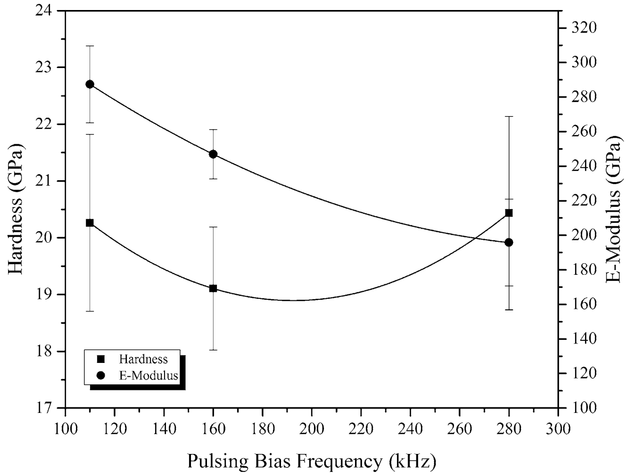

Fig. 5 Relationship between pulsing bias frequency, hardness and elastic modulus of $\mathbf{Cr_xN}$ films deposited at 90 V bias

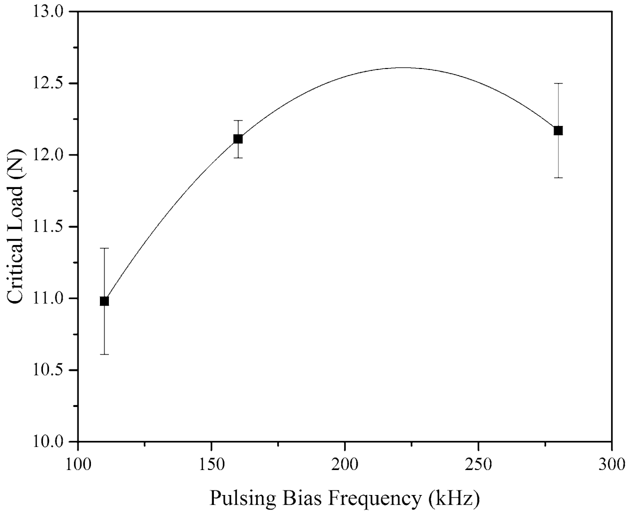

Fig. 6 Critical load for Cr_xN coatings deposited at different frequencies

Moreover, Cr_xN at 280 kHz depicted finer microstructure, which is a result of high ion bombardment during deposition process. Such microstructure is also associated with small grain size and high surface defects, which eventually result in high film hardness (Ref 35, 36). Lee et al. (Ref 15) observed a similar behavior of Cr_xN coatings for the 2-80 kHz frequency range. They reported that hardness reduced when bias frequency was increased to 50 kHz, and later showed a decrease in hardness. The authors attributed this to the availability of microstructure defects present within the coating.

3.5 Coating Adhesion

Pulsing of substrate bias in order to improve coating adhesion has been discussed by a number of authors (Ref 7, 29). They suggested that high additional energy could result from the ionized adatoms through the substrate bias, eventually leading to implantation of these ions into the substrate. This implantation would eventually influence the growth of deposited films, leading to better adhesion and mechanical

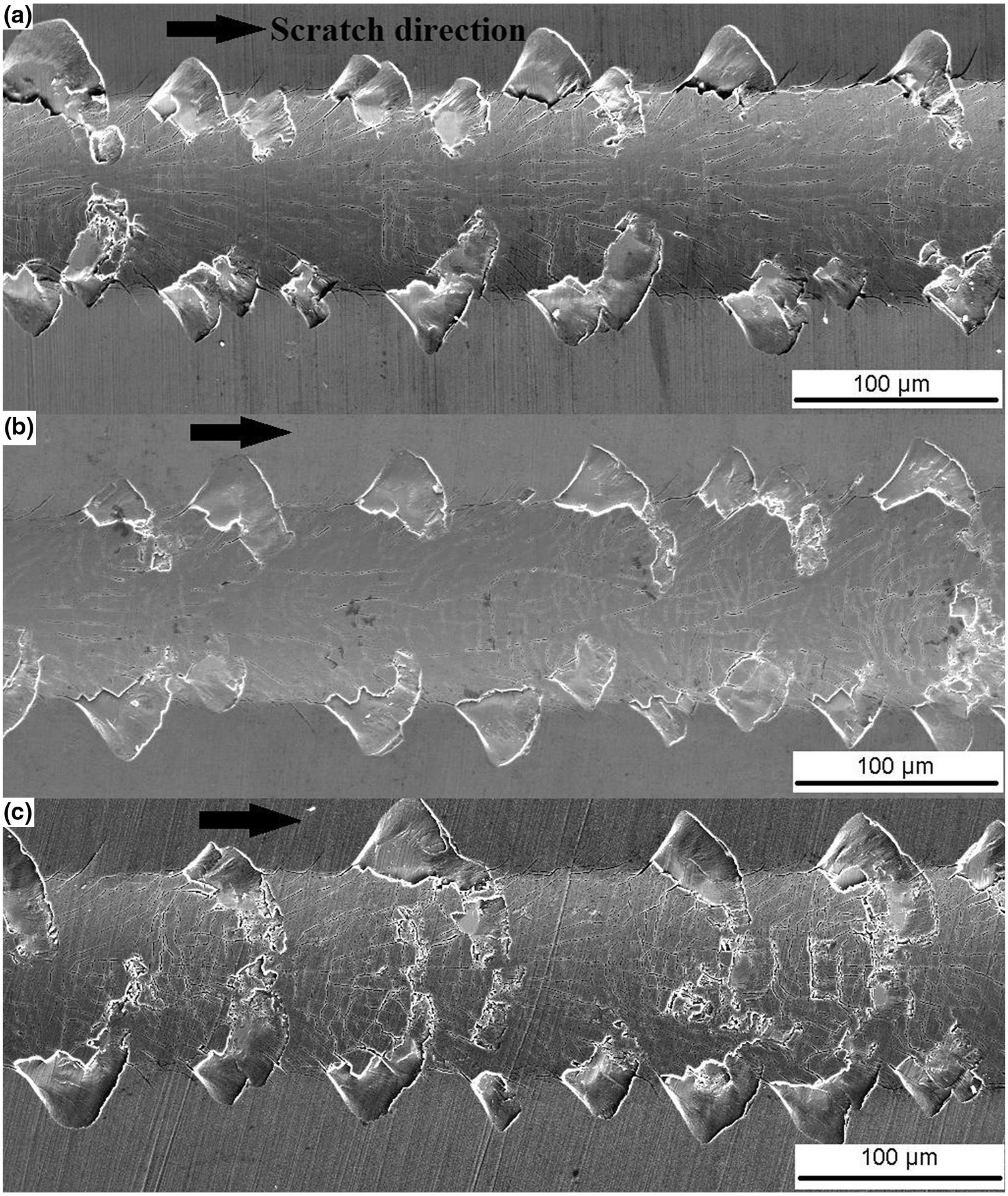

Fig. 7 SEM micrographs of scratch tracks on Cr_xN film deposited at: (a) 110 kHz, (b) 160 kHz and (c) 280 kHz

properties. In addition, these high-energy adatoms have greater mobility to find the low-energy wells on the surface to maximize adhesion (Ref 37). Therefore, it can be inferred that pulsed bias helps initiating secondary discharge at the substrate, which in turn reduced the residual stress and brittle fracture of the coating (Ref 29).

Adhesion analysis of the Cr_xN coatings was evaluated using scratch testing, shown in Fig. 6. The lowest critical load L_C (10.78 N) was measured for the Cr_xN deposited at 110 kHz, whereas at 160 kHz, the critical load increased to 12.15 N and remained constant for 280 kHz. Hence, coating adhesion is improved with the increase in substrate bias frequency.

SEM micrographs of the scratch tracks, on the samples with different bias frequencies (110, 160 and 280 kHz), are presented in Fig. 7(a-c). Almost similar failure mechanisms for all three coatings can be seen after scratch tests. Coating chipping/spallation occurs close to the scratch track, whereas large area chips (up to 40 μm in diameter) are removed.

For the coatings deposited at 110 and 160 kHz, the detachment of coating is observed at the edge of the track. Due to the sliding of stylus with an increasing load, tensile stresses are generated at the backside of the contact zone. When these stresses exceed the maximum surface and subsurface failure stresses, the generation of ring cracks is expected to take

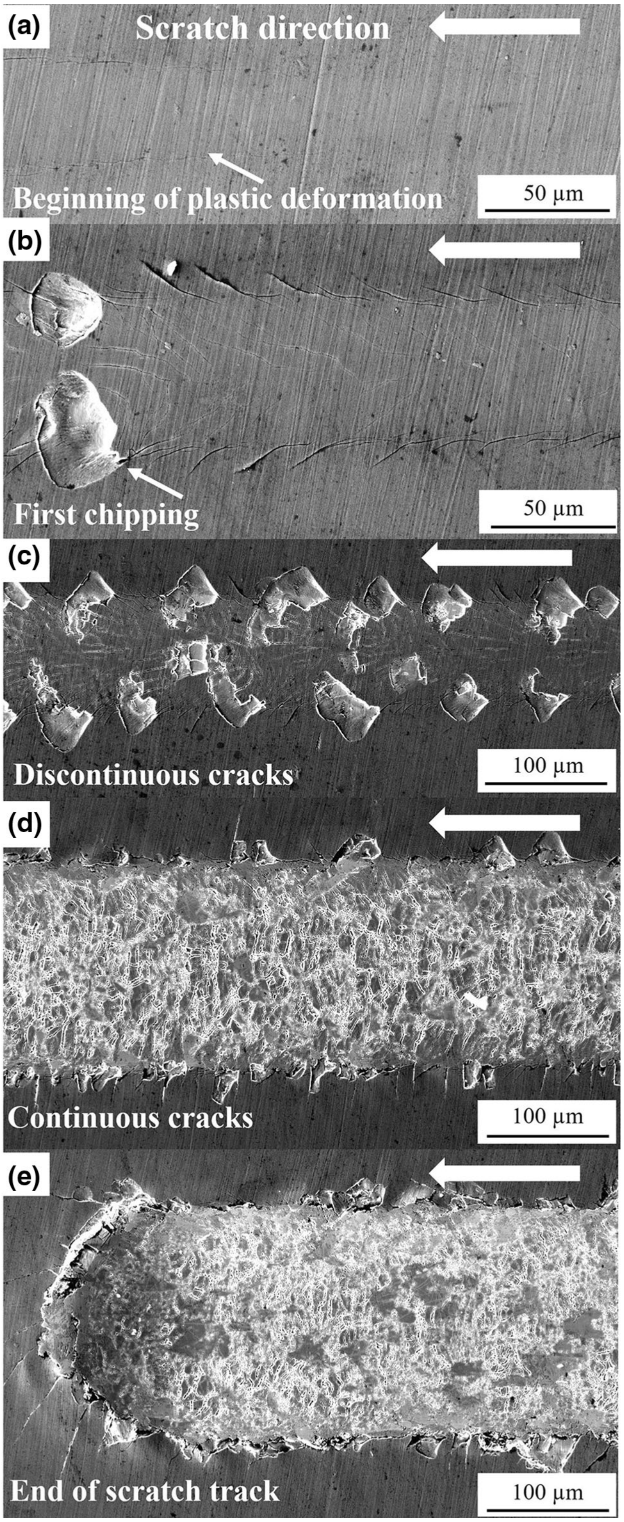

Fig. 8 SEM micrographs of scratch tracks on Cr_xN film deposited at 160 kHz

place at the subsurface zones. These ring cracks propagate with other asperities available within the coating, leading to full depth cracks or spallation of the coating in small pieces. This type of crack propagation is referred to as recovery spallation in the literature, as these cracks lead to stress recovery within the coating surface (Ref 38).

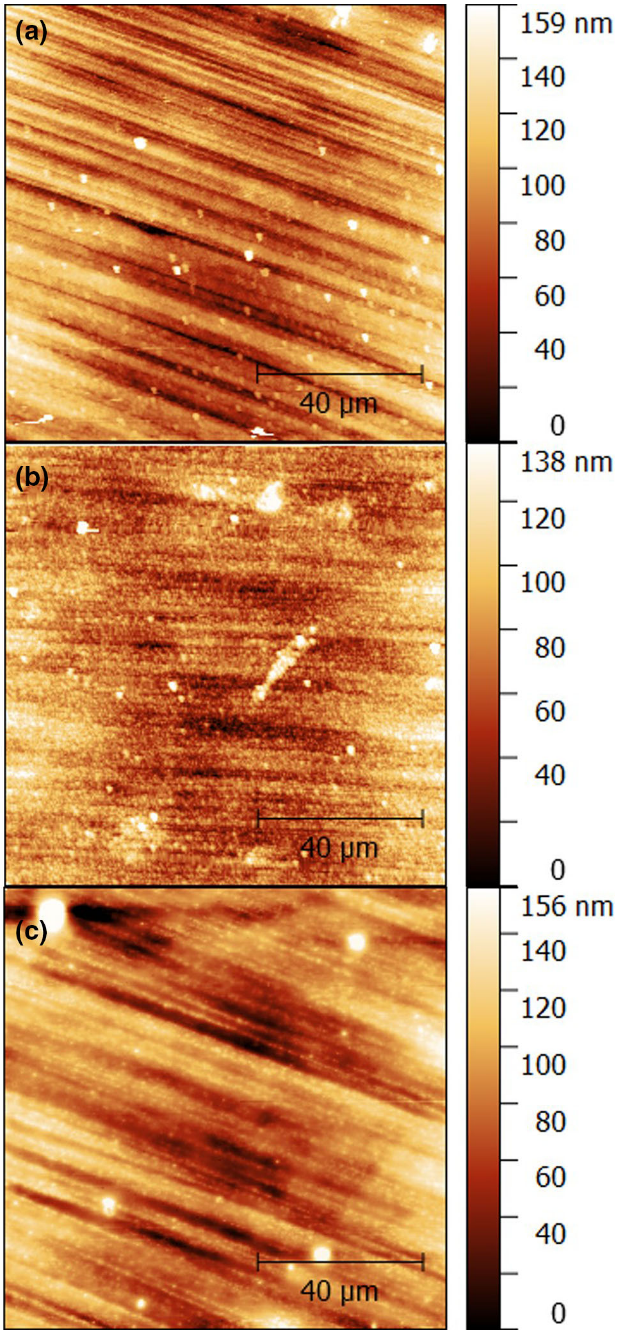

Fig. 9 Typical AFM images of Cr_xN film deposited at: (a) 110 kHz, (b) 160 kHz and (c) 280 kHz

A detailed analysis of the scratch tracks showing various coating spallation stages of Cr_xN coating deposited at 160 kHz is presented in Fig. 8(a-e). During the initial stages of scratch test, a transition from elastic to plastic deformation can be seen with the load increase (Fig. 8a). As the load increases further, chipping of the coating can be seen (Fig. 8b), which leads to a series of discontinuous cracks (Fig. 8c). In the later stages of the scratch tests, continuous cracks can be seen with complete removal of the coating (Fig. 8d, e).

Dominant spallation of the coating at the edges and within the track can be seen at 280 kHz in Fig. 7(c). Such type of spallation mechanism occurs due to high stresses in front of the stylus. Due to these compressive stresses, crack nucleation

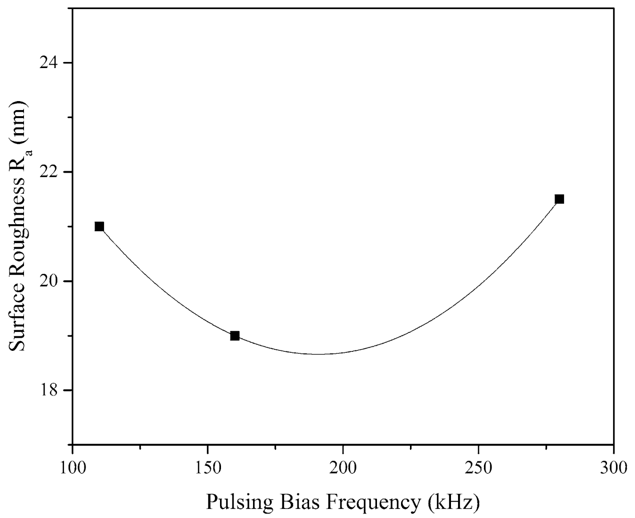

Fig. 10 Average surface roughness R_a for Cr_xN films deposited at different frequencies

takes place due to availability of interfacial flaws. These stresses relieve themselves in the form of spallation of coating within the track and outside of the track, referred to as compressive spallation (Ref 39). Increase in critical load is attributed to intensification of the Cr_2N phase, because the presence of the Cr_2N phase improves adhesion (Ref 40).

3.6 Surface Roughness

AFM images obtained from the Cr_xN films are shown in Fig. 9(a-c). It is clear from surface topography that all coatings exhibit similar microstructure with surface defects, which becomes larger with increasing substrate bias frequency.

Changes in the average surface roughness R_a of the Cr_xN films are illustrated in Fig. 10. For the Cr_xN coatings, general trend of increasing surface roughness can be observed. Low increase of approximately 2.5% of the surface roughness values has been observed between 110 and 280 kHz substrate frequencies. A rise in frequency leads to an increase in energy of the ions coming onto the substrate. Therefore, more nucleation sites occur on the coating surface leading to more surface defects and a rise in the coating roughness (Ref 30). A contrary observation was discussed by Lin et al. (Ref 14), where they reported a decrease in surface roughness with the increase in substrate frequency for the CrAlN coatings.

4. Conclusions

Cr_xN thin coatings were deposited at 110, 160 and 280 kHz bias frequencies at low duty cycle using pulsed DC reactive magnetron sputtering. Coating properties and microstructure were affected by the substrate bias frequency. Compact, dense and fine columnar structures were observed on the cross section of each coating. Increasing substrate frequency leads to finer and denser microstructure of the coatings. Experiments showed that pulsed DC bias of the Cr_xN films influences the phase formation within the films, resulting in high hardness (19-20 GPa) and improved adhesion. Additionally, an increase in surface roughness is observed with increased bias frequency.

Acknowledgments

We thank Mr. Sebastian Bolz for performing the WDS measurements, Mrs. Birgit Kunze for the sample preparation and metallographic analysis. A very special thanks to Mr. Frank Holländer for his technical support and cooperation during the experiments. We also thank Elena Uludintceva for assistance in proof-reading of this technical document.

References

1. P.J. Kelly and R.D. Arnell, Magnetron Sputtering: A Review of Recent Developments and Applications, *Vacuum*, 2000, **56**(3), p 159–172
2. M. Aliofkhazraei and N. Ali, 7.04 - PVD Technology in Fabrication of Micro- and Nanostructured Coating, *Comprehensive Materials Processing*, S.H.F.B.J.V.T. Yilbas, Ed., Elsevier, Oxford, 2014, p 49–84
3. P.J. Kelly and J.W. Bradley, Pulsed Magnetron Sputtering—Process Overview and Applications, *J. Optoelectron. Adv. Mater.*, 2009, **11**(9), p 1101–1107
4. E.B. Kashkarov, N. Nikitenkov, A.N. Sutygina, M.S. Syrtanov, O. Vilkhivskaya, T.S. Pryamushko, V. Kudiiarov, and L. Volesky, Effect of Titanium Ion Implantation and Deposition on Hydrogenation Behavior of Zr-1Nb Alloy, *Surf. Coat. Technol.*, 2016. doi:10.1016/j.surfcoat.2016.07.111
5. W.D. Sproul, Physical Vapor Deposition Tool Coatings, *Surf. Coat. Technol.*, 1996, **81**(1), p 1–7
6. E.B. Kashkarov, N.N. Nikitenkov, M.S. Syrtanov, A.N. Sutygina, I.A. Shulepov, and A.M. Lider, Influence of Plasma Immersion Titanium Implantation on Hydrogenation and Mechanical Properties of Zr–2.5Nb, *Appl. Surf. Sci.*, 2016, **370**, p 142–148
7. J.A. Freeman, P.J. Kelly, G.T. West, J.W. Bradley, and I. Iordanova, The Effects of Composition and Pulsed Biasing on Chromium Nitride Films, *Surf. Coat. Technol.*, 2009, **204**(6–7), p 907–910
8. P.H. Mayrhofer, H. Willmann, and C. Mitterer, Oxidation Kinetics of Sputtered Cr–N hard Coatings, *Surf. Coat. Technol.*, 2001, **146–147**, p 222–228
9. G.A. Zhang, P.X. Yan, P. Wang, Y.M. Chen, and J.Y. Zhang, Influence of Nitrogen Content on the Structural, Electrical and Mechanical Properties of CrN_x Thin Films, *Mater. Sci. Eng., A*, 2007, **460–461**, p 301–305
10. T. Hurkmans, D.B. Lewis, H. Paritong, J.S. Brooks, and W.D. Munz, Influence of Ion Bombardment on Structure and Properties of Unbalanced Magnetron Grown CrN_x Coatings, *Surf. Coat. Technol.*, 1999, **114**(1), p 52–59
11. D.-Y. Wang and K.-W. Weng, Deposition of CrN Coatings by Current-Modulating Cathodic arc Evaporation, *Surf. Coat. Technol.*, 2001, **137**(1), p 31–37
12. Z.B. Qi, B. Liu, Z.T. Wu, F.P. Zhu, Z.C. Wang, and C.H. Wu, A comparative Study of the Oxidation Behavior of Cr_2N and CrN Coatings, *Thin Solid Films*, 2013, **544**, p 515–520
13. C. Lorenzo-Martin, O. Ajayi, A. Erdemir, G.R. Fenske, and R. Wei, Effect of Microstructure and Thickness on the Friction and Wear Behavior of CrN Coatings, *Wear*, 2013, **302**(1–2), p 963–971
14. J. Lin, J.J. Moore, B. Mishra, M. Pinkas, W.D. Sproul, and J.A. Rees, Effect of Asynchronous Pulsing Parameters on the Structure and Properties of CrAlN Films Deposited by Pulsed Closed Field Unbalanced Magnetron Sputtering (P-CFUBMS), *Surf. Coat. Technol.*, 2008, **202**(8), p 1418–1436
15. J.-W. Lee, W.-C. Kuo, C.-J. Wang, L.-C. Chang, and K.-T. Liu, Effects of Substrate Bias Frequencies on the Characteristics of Chromium Nitride Coatings Deposited by Pulsed DC Reactive Magnetron Sputtering, *Surf. Coat. Technol.*, 2008, **203**(5–7), p 721–725
16. J.W. Bradley, H. Bäcker, Y. Aranda-Gonzalvo, P.J. Kelly, and R.D. Arnell, The Distribution of Ion Energies at the Substrate in an Asymmetric Bi-polar Pulsed DC Magnetron Discharge, *Plasma Sources Sci. Technol.*, 2002, **11**(2), p 165
17. S. Khamseh, M. Nose, T. Kawabata, A. Saiki, K. Matsuda, K. Terayama, and S. Ikeno, Effect of Deposition Conditions on the Structure and Properties of CrAlN Films Prepared by Pulsed DC Reactive Sputtering in FTS Mode at High Al Content, *Mater. Trans.*, 2008, **49**(9), p 2082–2090

18. W.C. Oliver and G.M. Pharr, An Improved Technique for Determining Hardness and Elastic Modulus using Load and Displacement Sensing Indentation Experiments, *J. Mater. Res.*, 1992, **7**(06), p 1564–1583
19. A. Lousa, J. Romero, E. Martınez, J. Esteve, F. Montala, and L. Carreras, Multilayered Chromium/Chromium Nitride Coatings for Use in Pressure Die-casting, *Surf. Coat. Technol.*, 2001, **146–147**, p 268–273
20. M. Naveed, A. Obrosov, and S. Weiß, Investigation of the Wear Resistance Properties of Cr/CrN Multilayer Coatings against Sand Erosion, *Conf. Pap. Sci.*, 2015, **2015**, p 9
21. R.L. Merlino, Understanding Langmuir Probe Current-Voltage Characteristics, *Am. J. Phys.*, 2007, **75**(12), p 1078–1085
22. P.J. Kelly, R. Hall, J. O'Brien, J.W. Bradley, G. Roche, and R.D. Arnella, Substrate Effects During Mid-frequency Pulsed DC Biasing, *Surf. Coat. Technol.*, 2001, **142–144**, p 635–641
23. R.D. Arnell, P.J. Kelly, J.W. Bradley, Control of Structure and Properties of Coatings Deposited by Pulsed Magnetron Sputtering, *Nanostructured Thin Films and Nanodispersion Strengthened Coatings*, A. Voevodin et al., Ed., Springer, Dordrecht, 2004, p 183–192
24. Y. Wei and C. Gong, Effects of Pulsed Bias Duty Ratio on Microstructure and Mechanical Properties of TiN/TiAlN Multilayer Coatings, *Appl. Surf. Sci.*, 2011, **257**(17), p 7881–7886
25. W. Olbrich, J. Fessmann, G. Kampschulte, and J. Ebberink, Improved Control of TiN Coating Properties Using Cathodic Arc Evaporation with a Pulsed Bias, *Surf. Coat. Technol.*, 1991, **49**(1–3), p 258–262
26. X.S. Wan, S.S. Zhao, Y. Yang, J. Gong, and C. Sun, Effects of Nitrogen Pressure and Pulse Bias Voltage on the Properties of Cr–N Coatings Deposited by Arc Ion Plating, *Surf. Coat. Technol.*, 2010, **204**(11), p 1800–1810
27. J. Lin, W.D. Sproul, J.J. Moore, S. Lee, and S. Myers, High Rate Deposition of Thick CrN and Cr_2N Coatings Using Modulated Pulse Power (MPP) Magnetron Sputtering, *Surf. Coat. Technol.*, 2011, **205**(10), p 3226–3234
28. G. Greczynski and L. Hultman, Time and Energy Resolved Ion Mass Spectroscopy Studies of the Ion Flux During High Power Pulsed Magnetron Sputtering of Cr in Ar and Ar/N2 Atmospheres, *Vacuum*, 2010, **84**(9), p 1159–1170
29. D. Bhaduri, A. Ghosh, S. Gangopadhyay, and S. Paul, Effect of Target Frequency, Bias Voltage and Bias Frequency on Microstructure and Mechanical Properties of Pulsed DC CFUBM Sputtered TiN Coating, *Surf. Coat. Technol.*, 2010, **204**(21–22), p 3684–3697
30. J.-W. Lee, S.-K. Tien, and Y.-C. Kuo, The Effects of Substrate Bias, Substrate Temperature, and Pulse Frequency on the Microstructures of Chromium Nitride Coatings Deposited by Pulsed Direct Current Reactive Magnetron Sputtering, *J. Electron. Mater.*, 2005, **34**(12), p 1484–1492
31. J. Lin, J.J. Moore, W.D. Sproul, B. Mishra, Z. Wu, and J. Wang, The Structure and Properties of Chromium Nitride Coatings Deposited Using dc, Pulsed DC and Modulated Pulse Power Magnetron Sputtering, *Surf. Coat. Technol.*, 2010, **204**(14), p 2230–2239
32. J. Lin, Z.L. Wu, X.H. Zhang, B. Mishra, J.J. Moore, and W.D. Sproul, A Comparative Study of CrN_x Coatings Synthesized by DC and Pulsed DC Magnetron Sputtering, *Thin Solid Films*, 2009, **517**(6), p 1887–1894
33. Z.G. Zhang, O. Rapaud, N. Bonasso, D. Mercs, C. Dong, C. Coddet, Control of Microstructures and Properties of DC Magnetron Sputtering Deposited Chromium Nitride Films, *Vacuum*, 2008, **82**(5), p 501–509
34. G. Bertrand, C. Savall, and C. Meunier, Properties of Reactively RF Magnetron-Sputtered Chromium Nitride Coatings, *Surf. Coat. Technol.*, 1997, **96**(2), p 323–329
35. J.E. Sundgren, Structure and Properties of TiN Coatings, *Thin Solid Films*, 1985, **128**(1), p 21–44
36. J.Y. Lee, Lifetime Improvement of Polymer Light Emitting Diodes Through a Poly(3,4-ethylenedioxythiophene): Silane Hole Transport Layer, *Chem. Phys. Lett.*, 2004, **393**(1–3), p 260–263
37. J. Sellers, Papers Presented at the Fifth International Conference on Plasma Surface Engineering Asymmetric bipolar Pulsed DC: The Enabling Technology for Reactive PVD, *Surface and Coatings Technology*, 1998, **98**(1), p 1245–1250
38. R.D. Arnell, The Mechanics of The Tribology of Thin Film Systems, *Surf. Coat. Technol.*, 1990, **43–44**(Part 2(0)), p 674–687
39. S.J. Bull, Failure Mode Maps in the Thin Film Scratch Adhesion Test, *Tribol. Int.*, 1997, **30**(7), p 491–498
40. X. Guan, Y. Wang, Q. Xue, and L. Wang, Toward High Load Bearing Capacity and Corrosion Resistance Cr/Cr_2N Nano-multilayer Coatings Against Seawater Attack, *Surf. Coat. Technol.*, 2015, **282**, p 78–85